Structural studies of -hairpin peptidomimetic antibiotics that target LptD in Pseudomonas sp

Schmidt, Jasmin ; Patora-Komisarska, Kristina ; Moehle, Kerstin ; Obrecht, Daniel ; Robinson, John A

Abstract: We report structural studies in aqueous solution on backbone cyclic peptides that possess potent antimicrobial activity specifically against Pseudomonas sp. The peptides target the -barrel outer membrane protein LptD, which plays an essential role in lipopolysaccharide transport to the outer membrane. The peptide L27-11 contains a 12-residue loop (T(1)W(2)L(3)K(4)K(5)R(6)R(7)W(8)K(9)K(10)A(11)K(12)) linked to a DPro-LPro template. Two related peptides were also studied, one with various Lys to ornithine or diaminobutyric acid substitutions as well as a DLys(6) (called LB-01), and another containing the same loop sequence, but linked to an LPro-DPro template (called LB-02). NMR studies and MD simulations show that L27-11 and LB-01 adopt -hairpin structures in solution. In contrast, LB-02 is more flexible and importantly, adopts a wide variety of different backbone conformations, but not -hairpin conformations. L27-11 and LB-01 show antimicrobial activity in the nanomolar range against Pseudomonas aeruginosa, whereas LB-02 is essentially inactive. Thus the -hairpin structure of the peptide is important for antimicrobial activity. An alanine scan of L27-11 revealed that tryptophan side chains (W(2)/W(8)) displayed on opposite faces of the -hairpin represent key groups contributing to antimicrobial activity.

DOI: https://doi.org/10.1016/j.bmc.2013.07.013

Structural Studies of ß-Hairpin Antibiotics that Target LptD in *Pseudomonas* sp.

Jasmin Schmidt[1], Kerstin Moehle[1], Daniel Obrecht[2] and John A. Robinson[1]*

[1]Chemistry Department, University of Zurich, Winterthurerstrasse 190, 8057 Zurich, Switzerland;

[2]Polyphor AG, Hegenheimermattweg 124, 5011 Allschwil

* Correspondence to:

Chemistry Department

University of Zurich

Winterthurestrasse 190

8057 Zurich

Switzerland

Tel: +41-44-6354242

E-mail: robinson@oci.uzh.ch

Abstract

We report structural studies in aqueous solution on a family of backbone cyclic peptides that possess potent antimicrobial activity specifically against *Pseudomonas* sp. These peptides target the ß-barrel outer membrane protein LptD, which plays an essential role in outer membrane biogenesis by translocating lipopolysaccharide molecules from the periplasm into the outer leaflet of the asymmetric outer membrane during cell growth. The cyclic lead peptide (L27-11) contains a 12-residue loop (TWLKKRRWKKAK) linked to a DPro-LPro template. Two related peptides were also studied, one with various Lys to ornithine or diaminobutyric acid (Dab) substitutions as well as a $D\text{Lys}^6$ (called LB-01), and another containing the same loop sequence as LB-01, but linked to an LPro-DPro template (called LB-02). NMR studies and MD simulations show that L27-11 and LB-01 adopt ß-hairpin structures in solution. However, the ß-strands and tip of the hairpin loop in L27-11 appear more flexible than with LB-01. LB-01 adopts a regular ß-hairpin structure in solution characterized by a consistent network of cross-strand NOEs and cross-strand hydrogen bonding interactions. In contrast, LB-02 appears more flexible and importantly, adopts a wide variety of different backbone ϕ/ψ angles but not ß-hairpin conformations. L27-11 and LB-01 both show antimicrobial activity in the nanomolar range against *P. aeruginosa*, whereas LB-02 is essentially inactive. Thus the ß-hairpin structure of the peptides appears to be very important for their antimicrobial activity. We surmise that a ß-hairpin-shaped peptide might be especially well suited to bind to proteins rich in ß-structure such as LptD in a membrane environment.

Introduction

A family of cyclic peptidomimetic antibiotics, represented by the cyclic peptide **L27-11** (Figure 1A), were reported recently to show potent antimicrobial activity against Gram-negative *Pseudomonas* sp.[1] The amino acid sequence of **L27-11** is unrelated to that of any known naturally occurring host-defense cationic antimicrobial peptide (CAP), although like many CAPs it does contain a mix of hydrophobic (aromatic) and cationic residues.[2] The peptidomimetics do not cause lysis of bacterial cell membranes, and only the enantiomer shown has antimicrobial activity in the nanomolar range against *Pseudomonas* sp.; the enantiomeric form is essentially inactive. Related molecules with optimized drug-like properties include **POL7001**, which has a much-improved stability towards proteolysis in human plasma due to the replacement of multiple Lys/Arg residues by diaminobutyric acid (Dab).[1] These substitutions do not have a large effect on antimicrobial activity, but remove cleavage sites for trypsin-like proteases. A related peptide called **POL7080** is now in clinical development, and has recently completed successfully a human phase I clinical trial.[3] A new narrow spectrum antibiotic targeting the important pathogen *P. aeruginosa* would be a welcome addition to the range of antibiotics currently available to treat serious hospital acquired infections, since life-threatening difficult-to-treat drug-resistant strains are arising with increasing frequency both in hospitals and in the wider community.[4]

These peptidomimetic antibiotics have a novel mechanism of action, involving an interaction with the outer membrane (OM) protein LptD.[1] The function of LptD in Gram-negative bacteria has been studied most thoroughly in *Escherichia coli*, where it plays an essential role in lipopolysaccharide (LPS) transport to the cell surface.[5] Seven essential Lpt (lipopolysaccharide transport) proteins are known to mediate LPS

transport from the inner membrane (IM), where the final steps of LPS assembly occur, to the outer leaflet of the asymmetric OM.[6] A heteromeric ABC transporter comprising the LptBFG complex in the IM, together with the lipoprotein LptC (Figure 1B) initiates LPS transport across the periplasm. LptC interacts with the soluble protein LptA, which in a head-to-tail oligomeric form likely creates a bridge across the periplasm.[7] LptD comprises a C-terminal ß-barrel domain embedded within the OM and an N-terminal domain that sits in the periplasm. The LptA bridge likely makes contact to the N-terminal periplasmic domain of LptD in the OM. This trans-envelope protein bridge provides a highway across which LPS molecules are shuttled from the IM to the OM in an ATP-dependent process (Figure 1B).[8] The lumen of the LptD ß-barrel domain appears to be at least partially occupied by a lipoprotein called LptE.[9] The LptD/E complex accepts LPS molecules from LptA in the periplasm and translocates them by an unknown mechanism into the outer leaflet. Upon exposure to **L27-11**, large accumulations of intracellular membrane-like material can be seen by transmission electron microscopy in *P. aeruginosa* cells.[1] Similar accumulations of membrane-like material are seen in *E. coli* and *P. aeruginosa* when *lptD*, or other essential genes in the Lpt pathway, are down-regulated, most likely due to the accumulation of LPS molecules in the IM.[5e, 10]

To aid understanding of how the peptidomimetic antibiotics interact with LptD, we report here NMR studies of the solution structure of the cyclic peptide **L27-11** (Figure 1A). This peptide contains a 12-residue loop (TWLKKRRWKKAK) coupled to a DPro-LPro template.[11] Two additional cyclic peptides have been studied (**LB-01** and **LB-02**, Figure 1A), with altered conformational properties in aqueous solution. In addition, evidence is presented that a ß-hairpin backbone conformation is very important for the antimicrobial activity of these peptides.

Results

Solution structure of L27-11

In water at pH 5.0, **L27-11** exists as a mixture of two slowly interconverting rotational isomers (rotamers) in 1:6 ratio arising from *cis-trans* isomerization at the Lys^{12}-DPro^{13} peptide bond. The two rotamers show characteristic ^{1}H-^{1}H NOEs between Lys^{12} Hα and DPro^{13} Hα (*cis*), or Lys^{12} Hα and DPro^{13} Hδ (*trans*), with the major form being *trans*. In a d_3-TFE/water (1/1 v/v) solution only the *trans* form was observed.

A complete assignment of ^{1}H and ^{13}C NMR spectra was only possible for the predominant *trans* rotamer of **L27-11** (see Supporting Information). Chemical shift deviations (CSDs) from statistical random coil values ($\Delta\delta=\delta^{observed} - \delta^{random}$) were determined for Hα, HN, Cα and Cβ resonances. CSDs can be sensitive indicators of secondary structure in peptides and proteins,[12] including ß-hairpins and ß-sheets.[13] Peptide backbone amide (HN) and Hα ^{1}H-CSDs are typically positive (downfield shifted) in ß-hairpins, whereas for ^{13}C-CSDs Cα values are negative and Cß positive. For **L27-11**, however, the residues predicted to occupy ß-strands (res. 1-5 and 7-12) show only very small HN and Hα ^{1}H-CSDs (Figure 2). The stronger upfield shift observed for Hα of Ala^{11} may be caused by an anisotropic effect from the Trp^{2} aromatic ring, which is predicted to lie in close proximity. Although the Cα ^{13}C-CSDs also do not display a clear trend, the Cβ CSDs, notably in residues 8-12 (Figure 2), do show larger positive values. A trend is also seen for CSDs at Arg^{6} and Arg^{7}, which occupy the turn position at the tip of the hairpin, with negative values of Hα and Cβ and positive values for HN and Cα, consistent with a ß-turn in this region.

$^3J_{HN\alpha}$ values are correlated with the backbone torsion angle ϕ via the Karplus relation and should be <6Hz in α-helices and >8Hz in β-sheets, whereas fast conformational averaging affords values close to 7Hz. The measured $^3J_{HN^\alpha}$ coupling constants (Figure 3) all lie in the range 6 - 8.1Hz, which might reflect fluctuations in the backbone torsion angle ϕ. Amide proton (HN) resonance temperature coefficients were measured, since $\Delta\delta_{NH}/T$ values lower (more positive) than about -5 ppb/K are expected for NH protons shielded from solvent and/or that are involved in intramolecular hydrogen bond formation.[14] NH temperature coefficients lower than -5 ppb/K were observed only for Thr[1], Leu[3], and Trp[8] at predicted hydrogen-bonding (HB) sites, as well as Arg[6] in the turn (Figure 3). Relative H/D exchange rates or amide protons in deuterated buffer were also measured, since relatively slow exchange could indicate intramolecular hydrogen bonding or shielding from the solvent. However, ^{1}H-NMR spectra measured in D_2O revealed rapid exchange (within minutes at 300 K) of all amide protons.

Analysis of NOESY plots revealed medium and long range NOEs characteristic of β-hairpin conformations, mostly for residues close to the DPro-LPro template (Figure 4). Unfortunately, resonance overlap for backbone and side-chain protons in lysine residues 4, 5 and 10 hindered the identification of specific NOE contacts to these residues. Some medium and long range NOEs characteristic of ß-hairpin structures are clearly seen, including Hα-Hα NOEs between Trp[2] and Ala[11], and Lys[4/5/10] and Lys[9], which would be expected between cross-strand residue pairs at non-hydrogen bonding (NHB) positions. In addition, cross-strand side-chain NOEs are seen between Trp[2]-Ala[11] and Trp[2]-Lys[9]. However, the absence of a more extensive network of cross-strand NOEs, and particularly the complete absence of cross-strand

NH-NH NOEs, is notable, and likely reflects partial melting of a regular hairpin structure. The available NOEs were used to derive distance restraints for structure calculations with DYANA (Table 1). The resulting average NMR structures, shown in Figure 4, could be superimposed with a backbone rmsd of 1.85 Å. This relatively large dispersion is characterized by fluctuations in the populated ϕ/ψ-angles. However, nascent ß-hairpin-like structures are readily discernible in all 20 NMR structures (Figure 4), mostly with distorted type-II ß-turns in Arg^6-Arg^7 at the tip.

In an effort to characterize the dynamic properties of the molecule, one typical NMR structure was used for a 100 ns MD simulation with time-averaged distance restraints in explicit solvent water at 300 K. An analysis of the resulting MD trajectory shows that the cyclic peptide remains predominantly in a ß-hairpin-like geometry, but shows increasing ϕ/ψ-angle fluctuations upon proceeding along both nascent ß-strands from the template (DPro-LPro) to the tip of the loop (Arg^6-Arg^7) (see Supporting Information). The distances between the Hα protons in residues at cross-strand NHB positions in regular anti-parallel ß-structure is in the range 2.2-2.5 Å. During the simulation, the mean Trp^2-Ala^{11} separation is 2.3±0.2Å, whereas the mean Lys^4-Lys^9 variation is significantly larger (3.1±0.6Å) (Figure 5). Residues Thr^1-Lys^5 and Trp^8-Lys^{12} adopt mostly extended ß-conformations (i.e. with $\phi = -120\pm20^o$ and $\psi = +130\pm20^o$), whereas at the tip of the hairpin Arg^6-Arg^7 adopts multiple different ß-turns during the simulation. As expected, the DPro-LPro template remains in a stable type-II' ß-turn conformation, with only small ϕ/ψ-angles fluctuations. During the MD simulation only two hydrogen bonds were significantly populated, between Thr^1 CO - Lys^{12} NH and Leu^3 NH – Lys^{10} CO, which correspond to cross-strand HB residues.

In summary, the structure and MD calculations suggest that **L27-11** populates nascent hairpin-like structures, with residues attached to the template being most strongly constrained into regular ß-structure, but with increasing backbone flexibility and melting of the backbone hairpin geometry towards the tip of the loop and with the absence of extensive cross-strand hydrogen bonding.

Solution structure of LB-01

Cyclic peptide **LB-01** is identical to **L27-11** except selected Lys residues have been substituted by Orn or Dab to facilitate full ^{1}H backbone and side-chain resonance assignments, and DLys is introduced at position-6 at the tip to stabilize a regular ß-hairpin conformation (Figure 1A). **LB-01** shows the same potent antimicrobial activity (MICs ≈ 0.01 μg/ml) against *Pseudomonas aeruginosa* as the lead **L27-11**. **LB-01** appears as a single rotamer (>98%) in aqueous solution, with all peptide bonds *trans*. A complete assignment of the ^{1}H NMR spectrum is given in the Supporting Information.

Analysis of CSDs shows a trend toward positive Hα and HN ^{1}H-CSDs (Figure 2), consistent with a hairpin structure. However, mostly small Cα ^{13}C-CSDs are observed. It should be noted that reference random coil values are not available for Dab and Orn. The random coil HN and Hα values for Lys were used for Orn and Dab residues, but the shortened side chain likely has a significant influence on the Cα and Cß ^{13}C-CSDs, and these are not included in Figure 2. The CSDs for DLys^{6} and Arg^{7} are consistent with a turn conformation at the tip of a hairpin. The large negative CSD for Hα Ala^{11} is again likely due to anisotropy effects from Trp^{2}. Analysis of coupling constants reveals $^{3}J_{HN\alpha}$ values for several residues ≥8.5 Hz (Figure 3), consistent with

extended backbone conformations. Moreover, H/D exchange experiments reveal several slowly exchanging amide protons, mostly at predicted cross-strand HB positions. The slower NH exchange seen for Trp^{2} might be due to shielding from the solvent by the aromatic side chain. Finally, the NH temperature coefficients of Thr^{1}, Orn^{5}, Orn^{9}, Dab^{10} and Lys^{12} show significantly lowered values.

In 2D NOESY plots for **LB-01**, numerous long-range cross-strand backbone and side chain NOEs are now seen (Figure 4). This network of cross-strand NOEs is a clear indication that regular ß-hairpin structures are populated in solution. Average structures calculated using NOE-derived distance restraints now converge to a narrow range of backbone torsion angles, with an rmsd of 0.47 Å (Figure 4 and Table 1). In the tip region ($DLys^{6}$-Arg^{7}) a type II' β-turn is found in all structures, consistent with characteristic Hα-HN and HN-HN NOEs between $DLys^{6}$-Trp^{8} and Arg^{7}-Trp^{8}, respectively. One typical NMR structure, in a MD simulation in a solvent water box with time-averaged distance restraints, now maintained ϕ/ψ backbone torsion angles in the β-region with only modest fluctuations over the entire simulation (see Supporting Information). The Hα-Hα distances between Trp^{2}-Ala^{11} and Dab^{4}-Orn^{9} remained 2.2±0.2 and 2.4±0.2 Å, respectively (Figure 5). The two turn regions ($DLys^{6}$-Arg^{7} and $DPro^{13}$-$LPro^{14}$) maintain ϕ/ψ angles typical of type-II' ß-turns. Analysis of hydrogen bonding during the MD simulation revealed a high population (80-90%) between Thr^{1} CO and Lys^{12} NH, Leu^{3} NH and Dab^{10} CO, Leu^{3} CO and Dab^{10} NH, Orn^{5} NH and Trp^{8} CO, as expected for cross-strand residues at HB sites. In summary, these results provide clear evidence that **LB-01** adopts a regular ß-hairpin structure in solution, characterized by a consistent network of cross-strand NOEs and with cross-strand hydrogen bonding interactions.

Solution structure of LB-02

In cyclic peptide **LB-02** (Figure 1A) the order of the heterochiral prolines in the template is changed to LPro[13]-DPro[14], which was expected to cause a major change in the entire backbone conformation compared to **LB-01**. **LB-02** shows no antimicrobial activity against *Pseudomonas sp*. (MIC ≥32 μg/ml). The ^{1}H NMR spectrum now reveals two rotamers in slow exchange due to *cis-trans* isomerism (≈ 1:2 ratio) at the LPro[13]-DPro[14] peptide bond. The major form is the *trans* rotamer, with a characteristic Hα-Hδ NOE, and the minor form is the *cis* rotamer, with a Hα-Hα NOE between Pro[13] and DPro[14]. Due to resonance overlap, unambiguous NMR assignments were only possible for the *trans* rotamer (see Supporting Information).

CSDs for *trans*-**LB-02** were mostly very small and reveal no consistent trend that would indicate regular secondary structure (Figure 2). Except for Thr[1], the majority of $^{3}J_{HN\alpha}$ values (Figure 3) lie in the range of 6.1-7.7 Hz, consistent with fast conformational averaging. All amide NH protons exchanged rapidly with solvent, although several amide NH temperature coefficients (-δΔ/ΔT) were smaller than 4.0, suggesting possible involvement in intramolecular hydrogen bonding or shielding from solvent. In 2D NOESY plots, most of the observed NOEs are intra-residue or sequential. Only a few weak medium range *i*, *i*+2 NOEs were seen, and none of the long-range cross-strand NOEs expected for regular β-hairpin structures were observed, except for residues directly attached to the LPro[13] – DPro[14] template (Figure 4).

With the available distance restraints, structure calculations were performed as for the previous examples, however, the resulting average structures revealed no

regular secondary structure. Upon superimposition of the 20 selected structures, mean backbone rmsd values were quite large (2.3 Å) (Table 1 and Figure 4). Characteristic NOEs (Thr^{1} HN - DPro^{14} Hδ, Thr^{1} HN - Pro^{13} Hα and Thr^{1} Hβ - Lys^{12} HN) around the Pro^{13} – DPro^{14} template suggest the formation of a type II β-turn in the major *trans* isomer, with torsion angles for Pro^{13} of $\phi = -58° \pm 3°$ and $\psi = 165° \pm 4°$ and for DPro^{14} of $\phi = 77° \pm 4°$ and $\psi = 18° \pm 44°$. However, there is no evidence for β-hairpin structures from residues 2 to 11.

An MD simulation in water solvent with time-averaged restraints was performed for one typical *trans* rotamer. Over the 100 ns simulation a wide range of interconverting backbone conformations were populated, with a deformed type II β-turn at the template and significant ϕ,ψ torsion angle fluctuations in the loop (see Supporting Information). Further analysis of the MD trajectory reveals the absence of any significant intramolecular hydrogen bonds. The Trp^{2}-Ala^{11} and Dab^{4}-Orn^{9} Hα-Hα distances (Figure 5) show significant fluctuations throughout the simulation, with average distances of 5.9 ± 0.7 Å and 14.0 ± 0.6 Å, respectively, which is much larger than expected for cross-strand residues in a ß-hairpin. The results reveal clearly that exchanging the sense of chirality of the Pro residues in the template, from **LB-01** to **LB-02**, has a profound effect on the backbone peptide conformation. Moreoever, **LB-02** exhibits considerable backbone flexibility but does not adopt hairpin-like conformations.

Circular Dichroism (CD)

The far-UV CD spectra of **L27-11**, **LB-01** and **LB-02** in aqueous solution are shown in Figure 6. Both **L27-11** and **LB-01** show a broad negative peak at 215 nm, although the mean residue ellipticity is higher for **LB-01**. In contrast, the shape of the CD curve for **LB-02** is quite different, showing that this peptide adopts (on the CD time scale) backbone conformations that are quite different from those present in **L27-11** and **LB-01**.

Discussion

The results reported here provide strong evidence that the cyclic peptides **L27-11** and **LB-01** adopt ß-hairpin structures in aqueous solution, whereas the related molecule **LB-02** adopts quite different backbone conformations. Structure calculations and MD simulations show that **LB-02** is quite flexible and adopts a wide variety of backbone ϕ/ψ angles but does not adopt ß-hairpin conformations. The UV-CD spectra of all three peptides (Figure 6), underscores the similarity between **L27-11** and **LB-01**, and the different structures populated by **LB-02**. The negative peak near 215 nm, with near to zero intensity at 200 nm, is close to that expected for a combination of antiparallel ß-sheets and type-II' ß-turns, whereas the weaker peaks and maxima observed for **LB-02** approximates more closely that expected for a random coil peptide.[15] The greater intensity of the band for **LB-02** compared to **L27-11** is also consistent with a more stable ß-hairpin conformation in the former.

L27-11 adopts a significant amount (ca. 17%) of the *cis*-rotamer at the Lys^{12}-D-Pro^{13} peptide bond. Since, however, only *trans*-peptide bonds are seen in **LB-01**, we can rule out that the antimicrobial activity of **L27-11** is associated specifically with the *cis*-rotamer. The NMR data for **L27-11** and **LB-01** provide a consistent

picture of their conformational behavior in solution. This view is based upon ^{1}H and ^{13}C CSDs, $^{3}J_{HN\alpha}$ values, temperature coefficients of amide protons, relative amide H-D exchange rates, and most importantly, observed NOE contacts. Both **L27-11** and **LB-01** adopt hairpin structures in solution. However, the ß-strands and tip of the hairpin loop in **L27-11** appear more flexible and likely have backbone ϕ/ψ angles that fluctuate more than with **LB-01**. This increased flexibility correlates with an apparent lack of stable cross-strand hydrogen bonding between the peptide amide groups of residue pairs at HB positions (i.e. residue pairs: 1=12, 3=10 and 5=8) of the hairpin. In contrast, the backbone flexibility in **LB-01** is lower, and this peptide now adopts stable ß-hairpin structures characterized by a significant extent of cross-strand hydrogen bonding between the residue pairs at HB positions. This difference in structure and dynamics is consistent with the hairpin stabilizing influence of a type-II' ß-turn at the tip of the hairpin, caused by introducing ^{D}Lys^{6}. A further important conclusion of this work is that the hairpin shape of **L27-11** and **LB-01** is very important for the antimicrobial activity. The complete loss of activity seen with **LB-02** correlates clearly with the massive change in backbone structure. Moreover, a linearized form of **L27-11** (Ac-PTWLKKRRWKKAL^{D}P-NH_2) is also devoid of antimicrobial activity. This conclusion is likely important for the ability of **L27-11** and **LB-01** to target the ß-barrel outer membrane protein LptD in *Pseudomonas* sp.[1] A ß-hairpin-shaped peptide might be especially well suited to bind to proteins rich in ß-structure, such as LptD. For example, the ß-strands in each ligand might interact with exposed edges of antiparallel ß-sheets in the ß-barrel target protein. Unfortunately no 3D structure of LptD is available to date, and the mechanism of LPS translocation to the cell surface promoted by LptD, is also unknown. Efforts are now underway to characterize the peptide-binding site in LptD in more detail.

Experimental Section

Peptide synthesis: The synthesis of **L27-11** was described earlier.[1] The peptides **LB-01** and **LB-02** were prepared and purified by HPLC in an identical manner (see Supporting Information).

NMR spectroscopy and structure calculations: ^{1}H NMR measurements were performed either in H_2O/D_2O (9:1), or pure D_2O at pH 5.0, or in a mixture (1:1) of trifluoroethanol (TFE-d_3) and H_2O/D_2O (9:1), pH 5.0. Spectra were acquired on *Bruker* AV-600 or AV-700 spectrometers at 300K. Water suppression was performed by presaturation. Spectral assignments were made by using 2D DQF-COSY, TOCSY, NOESY and ROESY spectra. Spectra were typically collected with 1024 x 256 complex data points zero-filled prior to Fourier transformation to 2048 x 1024, and transformed with a cosine-bell weighting function. $^{3}J_{HN\alpha}$ values were determined from 1D spectra or from 2D NOESY spectra by inverse Fourier transformation of in-phase multiplets. [^{13}C,^{1}H]-HSQC spectra at natural abundance were recorded in pure D_2O. Acquisition data were sampled as 1024 x 256 complex points, multiplied by a square-sine-bell window function and zero filled to 2 x 2 k points prior to Fourier transformation. All spectra were referenced using internal TSP standard. Distance restraints were obtained from NOESY and ROESY spectra with a mixing time of 250 ms. Data processing was carried out with TOPSPIN (*Bruker*) and XEASY.[16] The structure calculations were performed by restrained molecular dynamics in torsion angle space by applying the simulated annealing protocol implemented in the program DYANA.[17] Starting from 100 randomized conformations a bundle of 20 conformations is selected, which incur the lowest DYANA target energy function.

The program MOLMOL[18] was used for structure analysis and visualization of the molecular models. For measurement of CSDs, sequence corrections for the δ_{coil} values of Hα and Cα chemical shifts were implemented.[19]

Restrained MD simulations were carried out using GROMACS v4.5.4[20] with the OPLS force field in explicit solvent, applying periodic boundary conditions. The starting NMR structure was placed in a rhombic dodecahedral unit cell with a minimum distance of 0.9 nm to the box edge. SPC water molecules and ions to counterbalance the peptide charge were added yielding a final system of 2311 (**L27-11**), 2459 (**LB-01**) or 2420 (**LB-02**) water molecules and 7 chloride ions. Steepest decent minimization was performed. Electrostatics were treated with particle-mesh Ewald (PME) theory using a short range cut-off, and a cut-off for van der Waals forces of 1.0 nm. After 20 ps equilibration with position restraints on peptide heavy atoms, a 100 ns simulation with time averaged distance restraints was performed with a time step of 2 fs. In all simulations the temperature was maintained close to 300K by weak coupling to an external bath with a coupling constant of 0.1 ps. The pressure was kept constant at 1 bar by coupling the system (τ=2 ps) to a pressure bath. The LINCS algorithm was used to constrain all bond lengths.

The NMR structures of **L27-11** and **LB-01** have been deposited in the PDB databank under the accession numbers XXX and XXX, respectively.

CD spectroscopy

The CD were measured using a Jasco J-175 spectrometer equipped with a temperature controller using a quartz cell of 1 cm path length. The spectra were recorded at 283K from 195 to 260 nm, at 0.5 nm resolution with a scan rate of 5 nm/min and a sensitivity of 50 mdeg. Three scans were accumulated and averaged for each

spectrum. Raw data were manipulated by smoothing and subtraction of solvent spectra. CD values were expressed as the mean residue molar ellipticity.

Acknowledgements

The authors thank the Swiss National Science Foundation for supporting this work.

References

[1] N. Srinivas, P. Jetter, B. J. Ueberbacher, M. Werneburg, K. Zerbe, J. Steinmann, B. Van der Meijden, F. Bernardini, A. Lederer, R. L. A. Dias, P. E. Misson, H. Henze, J. Zumbrunn, F. O. Gombert, D. Obrecht, P. Hunziker, S. Schauer, U. Ziegler, A. Kach, L. Eberl, K. Riedel, S. J. DeMarco, J. A. Robinson, *Science* **2010**, *327*, 1010-1013.

[2] a) L. T. Nguyen, E. F. Haney, H. J. Vogel, *Trends Biotechnol*. **2011**, *29*, 464-472; b) N. Y. Yount, M. R. Yeaman, in *Ann. Rev. Pharmacol. Toxicol., Vol. 52* (Eds.: P. A. Insel, S. G. Amara, T. F. Blaschke), Annual Reviews, Palo Alto, **2012**, pp. 337+.

[3] D. T. Moir, T. J. Opperman, M. M. Butler, T. L. Bowlin, *Curr. Opin. Pharmacol*. **2012**, *12*, 535-544.

[4] H. W. Boucher, G. H. Talbot, J. S. Bradley, J. E. Edwards, D. Gilbert, L. B. Rice, M. Scheld, B. Spellberg, J. Bartlett, *Clin. Infect. Dis*. **2009**, *48*, 1-12.

[5] a) M. P. Bos, B. Tefsen, J. Geurtsen, J. Tommassen, *Proc. Natl. Acad. Sci. USA* **2004**, *101*, 9417-9422; b) M. Braun, T. J. Silhavy, *Mol. Microbiol*. **2002**, *45*, 1289-1302; c) S.-S. Chng, N. Ruiz, G. Chimalakonda, T. J. Silhavy, D.

Kahne, *Proc. Natl. Acad. Sci. USA* **2010**, *107*, 5363-5368; d) P. Sperandeo, G. Dehó, A. Polissi, *Biochim. Biophys. Acta* **2009**, *1791*, 594-602; e) T. Wu, A. C. McCandlish, L. S. Gronenberg, S.-S. Chng, T. J. Silhavy, D. Kahne, *Proc. Natl. Acad. Sci. USA* **2006**, *103*, 11754-11759.

[6] a) M. P. Bos, V. Robert, J. Tommassen, *Annu. Rev. Microbiol.* **2007**, *61*, 191-214; b) N. Ruiz, D. Kahne, T. J. Silhavy, *Nat. Rev. Microbiol.* **2009**, *7*, 677-683.

[7] S. S. Chng, L. S. Gronenberg, D. Kahne, *Biochemistry* **2010**, *49*, 4565-4567.

[8] S. Okuda, E. Freinkman, D. Kahne, *Science* **2012**.

[9] E. Freinkman, S. S. Chng, D. Kahne, *Proc. Nat. Acad. Sci. USA* **2011**, *108*, 2486-2491.

[10] M. Werneburg, K. Zerbe, M. Juhas, L. Bigler, U. Stalder, A. Kaech, U. Ziegler, D. Obrecht, L. Eberl, J. A. Robinson, *ChemBioChem* **2012**, *13*.

[11] J. A. Robinson, *Accts. Chem. Res.* **2008**, *41*, 1278-1288.

[12] a) D. S. Wishart, C. G. Bigam, A. Holm, R. S. Hodges, B. D. Sykes, *J. Biomol. NMR* **1995**, *5*, 67-81; b) J. Makowska, S. Rodziewicz-Motowidło, K. Bagińska, J. A. Vila, A. Liwo, L. Chmurzyński, H. A. Scheraga, *Proc. Nat. Acad. Sci. USA* **2006**, *103*, 1744-1749; c) D. S. Wishart, *Prog. Nucl. Mag. Res. Spectr.* **2011**, *58*, 62-87.

[13] a) G. J. Sharman, S. R. Griffiths-Jones, M. Jourdan, M. S. Searle, *J. Am. Chem. Soc.* **2001**, *123*, 12318-12324; b) I. Shu, J. M. Stewart, M. Scian, B. L. Kier, N. H. Andersen, *J. Am. Chem. Soc.* **2011**, *133*, 1196-1199; c) R. M. Fesinmeyer, F. M. Hudson, K. A. Olsen, G. W. N. White, A. Euser, N. H. Andersen, *J. Biomol. NMR* **2005**, *33*, 213-231.

[14] a) N. J. Baxter, M. P. Williamson, *J. Biomol. NMR* **1997**, *9*, 359-369; b) T. Cierpicki, J. Otlewski, *J. Biomol. NMR* **2001**, *21*, 249-261.

[15] N. J. Greenfield, *Nature Protocols* **2004**, *1*, 2876-2890.

[16] C. Bartels, T.-h. Xia, M. Billeter, P. Güntert, K. Wüthrich, *J. Biomol. NMR* **1995**, *6*, 1-10.

[17] P. Guntert, C. Mumenthaler, K. Wuthrich, *J. Mol. Biol.* **1997**, *273*, 283-298.

[18] R. Koradi, M. Billeter, K. Wuthrich, *J. Mol. Graph.* **1996**, *14*, 51-55.

[19] S. Schwarzinger, G. J. A. Kroon, T. R. Foss, J. Chung, P. E. Wright, H. J. Dyson, *J. Am. Chem. Soc.* **2001**, *123*, 2970-2978.

[20] B. Hess, C. Kutzner, D. van der Spoel, E. Lindahl, *J. Chem. Theory Comp.* **2008**, *4*, 435-447.

Figure Legends

Figure-1. **A**, Structures of the cyclic peptidomimetic antibiotics. Orn = L-ornithine, Dab = L-diaminobutyric acid, DK = DLys. **B**, The peptidomimetic antibiotics target LptD, an OM protein essential for LPS transport to the cell surface (see text).

A

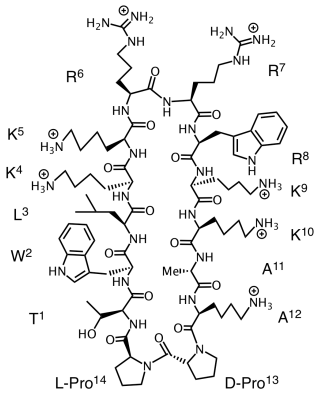

L27-11

mimetic	position													
	1	2	3	4	5	6	7	8	9	10	11	12	13	14
L27-11	T	W	L	K	K	R	R	W	K	K	A	K	DP	P
LB-01	T	W	L	Dab	Orn	DK	R	W	Orn	Dab	A	K	DP	P
LB-02	T	W	L	Dab	Orn	DK	R	W	Orn	Dab	A	K	P	DP

B

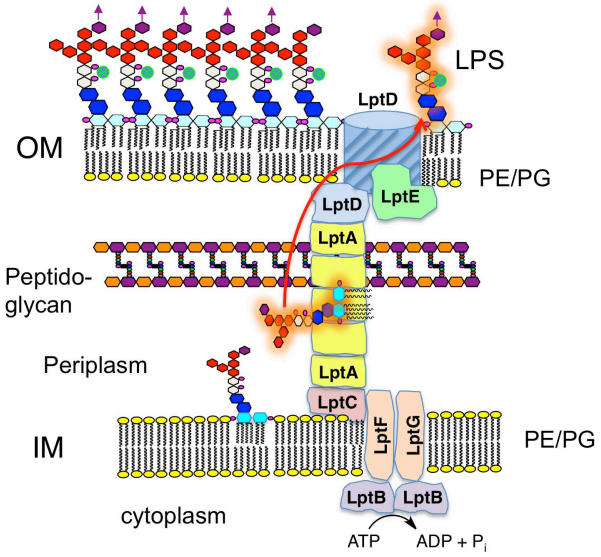

Figure 2. NMR Chemical shift deviations (CSDs) ($\Delta\delta = \delta^{observed} - \delta^{random}$) for Hα, HN, Cα and Cβ,[12a, 12b, 19] for residues 1-12 in peptides **L27-11**, **LB-01** and **LB-02**. Note, ^{13}C-CSDs are not displayed for Orn and Dab residues (4, 5, 9 and 10) in **LB-01** and **LB-02**.

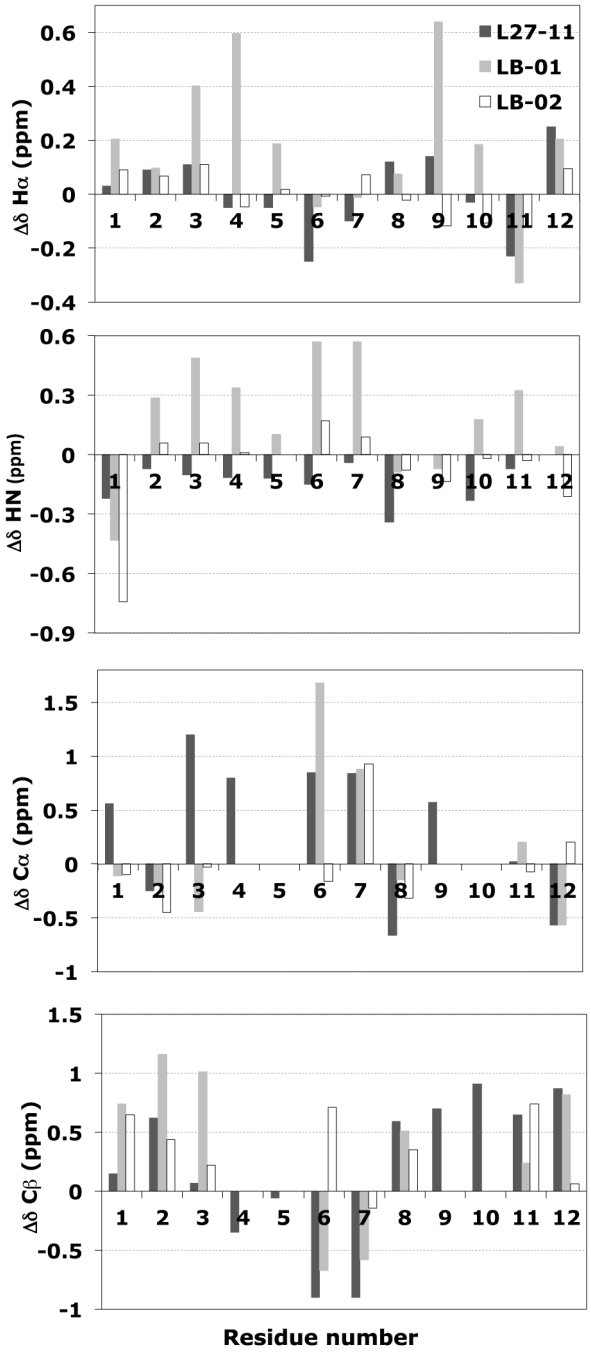

Figure 3. Coupling constants, temperature coefficients of amide NH resonances, and relative peptide NH exchange rates (open circle = fast, half filled = slower, filled = slowest) for residues 1-12 in each peptide.

		residue											
		1	2	3	4	5	6	7	8	9	10	11	12
L27-11	$^3J_{\alpha N}$	8.0	8.0	7.0	nd	nd	nd	nd	7.6	7.0	8.1	6.9	nd
	-δΔ/ΔT [ppb/K]	4.2	8.0	1.8	6.4	6.4	4	6.9	4.7	6.1	5.7	5.6	6.6
	k_{exch}	○	○	○	○	○	○	○	○	○	○	○	◐
LB-01	$^3J_{\alpha N}$	8.5	8.1	8.7	8.8	7.6	4.7	7.1	7.6	8.1	7.6	6.0	9.1
	-δΔ/ΔT [ppb/K]	2.0	8.7	6.9	6.8	3.5	8.7	8.9	5.1	3.7	4.1	7.4	3.5
	k_{exch}	◐	◐	●	○	○	○	○	●	○	○	○	●
LB-02	$^3J_{\alpha N}$	9.0	7.7	7.4	7.4	nd	6.7	7.4	6.8	7.3	6.4	6.1	6.8
	-δΔ/ΔT [ppb/K]	1.8	9.4	9.4	6.4	8.4	7.5	6.4	9.0	1.9	6.1	7.1	7.1
	k_{exch}	○	○	○	○	○	○	○	○	○	○	○	○

(nd – determination not possible due to significant resonance overlap)

Figure 4. Dotted arrows indicate long range NOEs observed for **L27-11**, **LB-01** and **LB-02** (red arrow on **L27-11** indicates NOE that cannot be unambiguously assigned due to signal overlap (see text); red arrow on **LB-01** indicates an NOE that should be observable, but was not detected due to insufficient separation of resonances); the resulting bundle of 20 average solution structures for each peptide; and one representative structure for **LB-01** (template in light brown/blue).

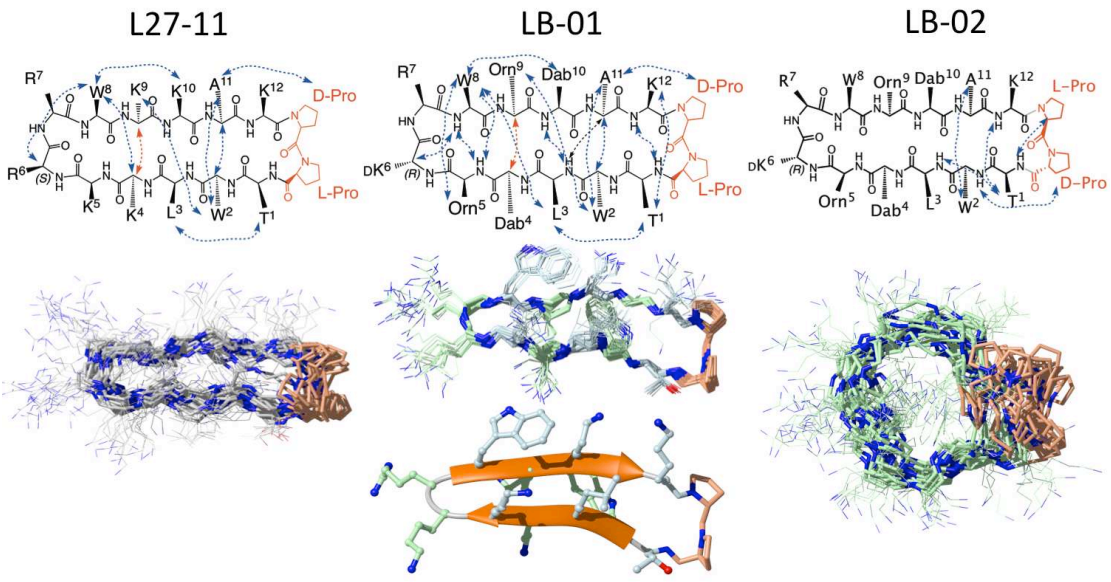

Figure 5. The distance separation (Å) of the Hα atoms of residues 2 and 11, and 4 and 9, during the 100 ns restrained MD simulations for **L27-11**, **LB-01** and **LB-02**.

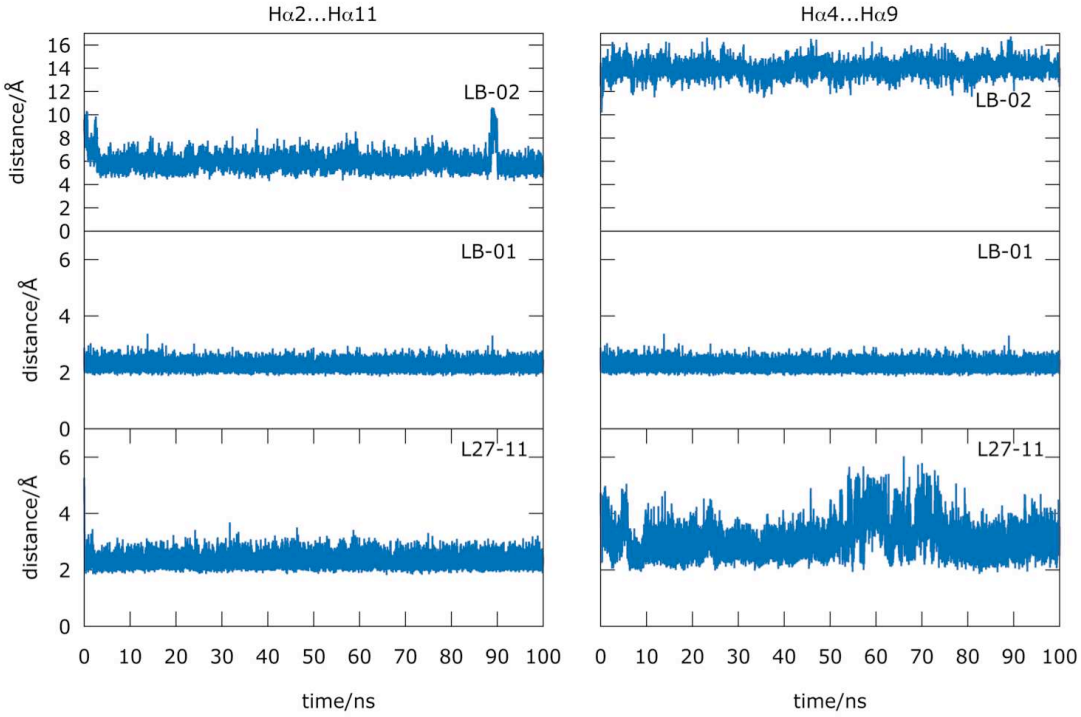

Figure 6. UV-CD spectra recorded for **L27-11**, **LB-01** and **LB-02** in water pH 5.0 at 298 K.

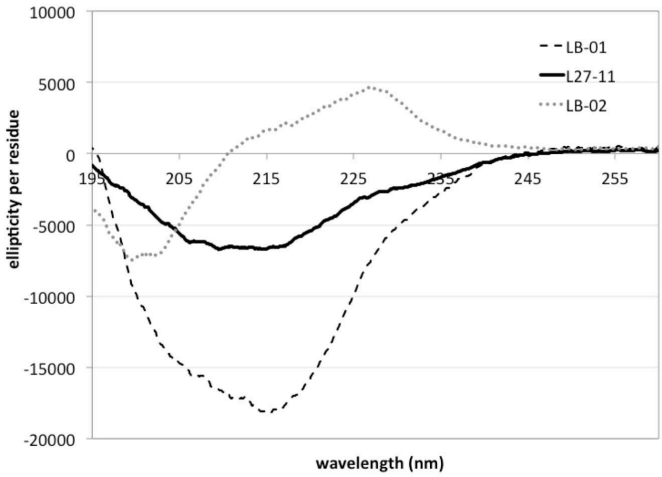

Table 1. Summary of statistics for the final 20 NMR structures calculated using DYANA for **L27-11**, **LB-01** and **LB-02**.

	L27-11	**LB-01**	**LB-02**
Number of NOE upper-distance limits	74	181	86
Intraresidue	27	49	38
Sequential	33	44	39
Medium- and long-range	14	48	9
Residual target function value ($Å^2$)	0.57 ± 0.08	0.62 ± 0.05	0.48 ± 0.05
Mean rmsd values (Å)			
All backbone atoms	1.85 ± 0.51	0.47 ± 0.21	2.32 ± 0.63
All heavy atoms	3.65 ± 0.92	1.27 ± 0.21	4.44 ± 0.22
Residual NOE violations			
Number > 0.2 Å	8	5	4
Maximum (Å)	0.33	0.25	0.0

Graphical abstract

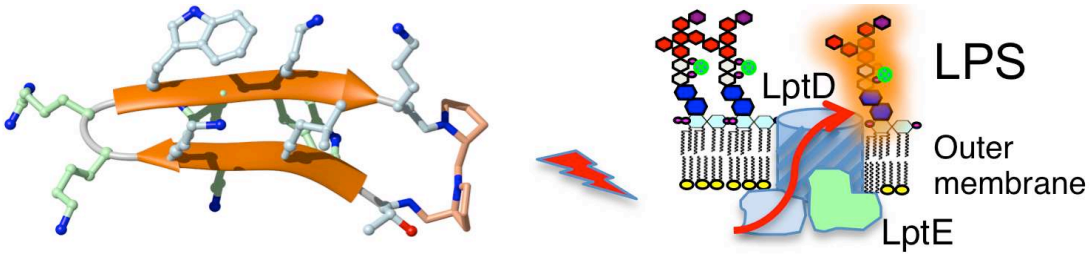

Cyclic antimicrobial peptides targeting the lipopolysaccharide translocator LptD/E in *Pseudomonas* sp. are shown to adopt ß-hairpin conformations in solution. This folded structure is important for the antibacterial activity.

Keywords

Antibacterial, conformation, peptide, peptidomimetic, Pseudomonas aeruginosa, lipopolysaccharide transport, ß-barrel membrane protein.

Supporting Information

1. Peptide synthesis

The synthesis of **L27-11** was described earlier (ref. [1]). The peptides **LB-01** and **LB-02** were synthesized and purified in the same way.

Masses of the peptides **LB-01** and **LB-02** by electrospray MS (positive ion mode), and retention time (t_R) on analytical HPLC (column: *Agilent Zorbax Eclipse* XDB-C18, flow rate: 1 mL/min, linear gradient: 10 to 50 % MeCN in water with 0.1 % TFA in 3 column volumes) are given below. The peptides were ≥98% pure by analytical HPLC.

Mimetic	Chemical formula	m/z		t_R [min]
		obs.	M^+ calc.	
LB-01	$C_{81}H_{129}N_{25}O_{15}$	1693.0	1692.01	9.47
LB-02	$C_{81}H_{129}N_{25}O_{15}$	1693.0	1692.01	9.80

2. NMR proton chemical shift assignments

L27-11

	NH	H-C(α)	H-C(β)	Others
Thr[1]	7.93	4.29	4.21	CH_3(γ) 1.19
Trp[2]	8.18	4.75	3.10, 3.23	H(δ^1) 7.21; H(ε^3) 7.47; H(ζ^2) 7.50; H(ζ^3) 7.10; H(η^2) 7.23; NH(ε^1) 10.13
Leu[3]	8.06	4.29	1.49, 1.49	CH(γ) 1.39; CH_3(δ) 0.83, 0.88
Lys[4]	8.17	4.28	nd	CH_2(γ) nd; CH_2(δ) nd; CH_2(ε) 2.88, 2.88; CH_3(ζ) 7.50
Lys[5]	8.17	4.28	1.69, 1.83	CH_2(γ) nd; CH_2(δ) nd; CH_2(ε) 2.89, 2.89; CH_3(ζ) 7.51
Arg[6]	8.14	4.11	1.72, 1.72	CH_2(γ) 1.49, 1.54; CH_2(δ) 3.10, 3.10; NH(ε) 7.13; NH_2(η) -, -
Arg[7]	8.19	4.17	1.67, 1.73	CH_2(γ) 1.36, 1.39; CH_2(δ) 3.05, 3.05; NH(ε) 7.07; NH_2(η) -, -
Trp[8]	7.91	4.78	3.24, 3.36	H(δ^1) 7.26; H(ε^3) 7.60; H(ζ^2) 7.51; H(ζ^3) 7.13; H(η^2) 7.24; NH(ε^1) 10.23
Lys[9]	8.29	4.46	1.69, 1.78	CH_2(γ) 1.31, 1.31; CH_2(δ) 1.48, 1.53; CH_2(ε) 2.79, 2.79; CH_3(ζ) 7.41
Lys[10]	8.06	4.28	1.51, 1.73	CH_2(γ) 1.35, 1.35; CH_2(δ) 1.65, 1.65; CH_2(ε) 2.96, 2.96; CH_3(ζ) 7.54
Ala[11]	8.17	4.11	1.18	
Lys[12]	8.18	4.70	1.59, 1.73	CH_2(γ) 1.30, 1.36; CH_2(δ) 1.58, 1.58; CH_2(ε) 2.88, 2.88; CH_3(ζ) -
Dpro[13]	-	4.73	1.92, 2.30	CH_2(γ) 2.00, 2.07; CH_2(δ) 3.54, 3.69
Pro[14]		4.42	1.91, 2.15	CH_2(γ) 1.96, 2.04; CH_2(δ) 3.69, 3.90

LB-01

	NH	H-C(α)	H-C(β)	Others
Thr[1]	7.72	4.21	4.16	CH_3(γ) 1.18
Trp[2]	8.54	4.75	3.04, 3.04	H(δ^1) 7.22; H(ε^3) 7.30; H(ζ^2) 7.49; H(ζ^3) 7.00; H(η^2) 7.23; NH(ε^1) 10.16
Leu[3]	8.65	4.55	1.64, 1.64	CH(γ) 1.53; CH_3(δ) 0.88, 0.90
Dab[4]	8.63	4.92	2.04, 2.13	CH_2(γ) 2.82, 2.94; CH_3(δ) 7.66
Orn[5]	8.39	4.48	1.78, 1.89	CH_2(γ) 1.64, 1.71; CH_2(δ) 2.95, 2.95; CH_3(ε) 7.59
DLys[6]	8.86	4.26	1.76, 1.76	CH_2(γ) 1.35, 1.48; CH_2(δ) 1.69, 1.69; CH_2(ε) 2.97, 2.97; CH_3(ζ) 7.56
Arg[7]	8.80	4.20	1.57, 1.70	CH_2(γ) 1.29, 1.35; CH_2(δ) 3.04, 3.04; NH(ε) 7.05; NH_2(η) -, -
Trp[8]	8.16	4.73	3.27, 3.45	H(δ^1) 7.33; H(ε^3) 7.54; H(ζ^2) 7.48; H(ζ^3) 7.03; H(η^2) 7.20; NH(ε^1) 10.13
Orn[9]	8.22	4.89	1.70, 1.81	CH_2(γ) 1.58, 1.61; CH_2(δ) 2.56, 2.70; CH_3(ε) 7.35
Dab[10]	8.47	4.45	1.83, 2.02	CH_2(γ) 2.82, 2.97; CH_3(δ) 7.76
Ala[11]	8.56	3.98	0.89	
Lys[12]	8.22	4.61	1.48, 1.70	CH_2(γ) 1.25, 1.35; CH_2(δ) 1.63, 1.63; CH_2(ε) 2.92, 2.92; CH_3(ζ) 7.54
Dpro[13]	-	4.69	1.85, 2.25	CH_2(γ) 1.95, 2.04; CH_2(δ) 3.39, 3.68
Pro[14]		4.44	2.03, 2.13	CH_2(γ) 1.90, 2.03; CH_2(δ) 3.66, 3.92

LB-02 (major trans form)

	NH	H-C(α)	H-C(β)	Others
Thr[1]	7.41	4.34	4.09	CH_3(γ) 1.09
Trp[2]	8.32	4.73	3.11, 3.25	H(δ^1) 7.20; H(ε^3) 7.59; H(ζ^2) 7.46; H(ζ^3) 7.11; H(η^2) 7.20; NH(ε^1) 10.11
Leu[3]	8.22	4.30	1.50, 1.50	CH(γ) 1.49; CH_3(δ) 0.81, 0.81
Dab[4]	8.30	4.27	1.97, 2.13	CH_2(γ) 2.86, 2.97; CH_3(δ) -
Orn[5]	8.29	4.34	1.77, 1.88	CH_2(γ) 1.70, 1.70; CH_2(δ) 2.99, 2.99; CH_3(ε) -
DLys[6]	8.46	4.31	1.74, 1.78	CH_2(γ) 1.34, 1.41; CH_2(δ) 1.62, 1.62; CH_2(ε) 2.90, 2.90; CH_3(ζ) -
Arg[7]	8.32	4.31	1.62, 1.69	CH_2(γ) 1.41, 1.41; CH_2(δ) 3.07, 3.07; NH(ε) 7.09; NH_2(η) -, -
Trp[8]	8.17	4.64	3.15, 3.26	H(δ^1) 7.17; H(ε^3) 7.53; H(ζ^2) 7.47; H(ζ^3) 7.10; H(η^2) 7.22; NH(ε^1) 10.06
Orn[9]	8.16	4.20	1.68, 1.82	CH_2(γ) 1.62, 1.62; CH_2(δ) 2.96, 2.96; CH_3(ε) -
Dab[10]	8.27	4.21	2.00, 2.12	CH_2(γ) 2.99, 2.99; CH_3(δ) -
Ala[11]	8.21	4.20	1.31	
Lys[12]	8.97	4.53	1.60, 1.75	CH_2(γ) 1.26, 1.41; CH_2(δ) 1.62, 1.62; CH_2(ε) 2.90, 2.90; CH_3(ζ) -

Pro[13]	-	4.55	1.79, 2.31	$CH_2(\gamma)$ 2.02, 2.10; $CH_2(\delta)$ 3.59, 3.84
DPro[14]		4.44	1.80, 2.10	$CH_2(\gamma)$ 1.38, 1.78; $CH_2(\delta)$ 3.40, 3.60

^{1}H-NMR spectrum of **L27-11** (700 MHz, H_2O/D_2O = 9:1, pH 5.0, 298 K).

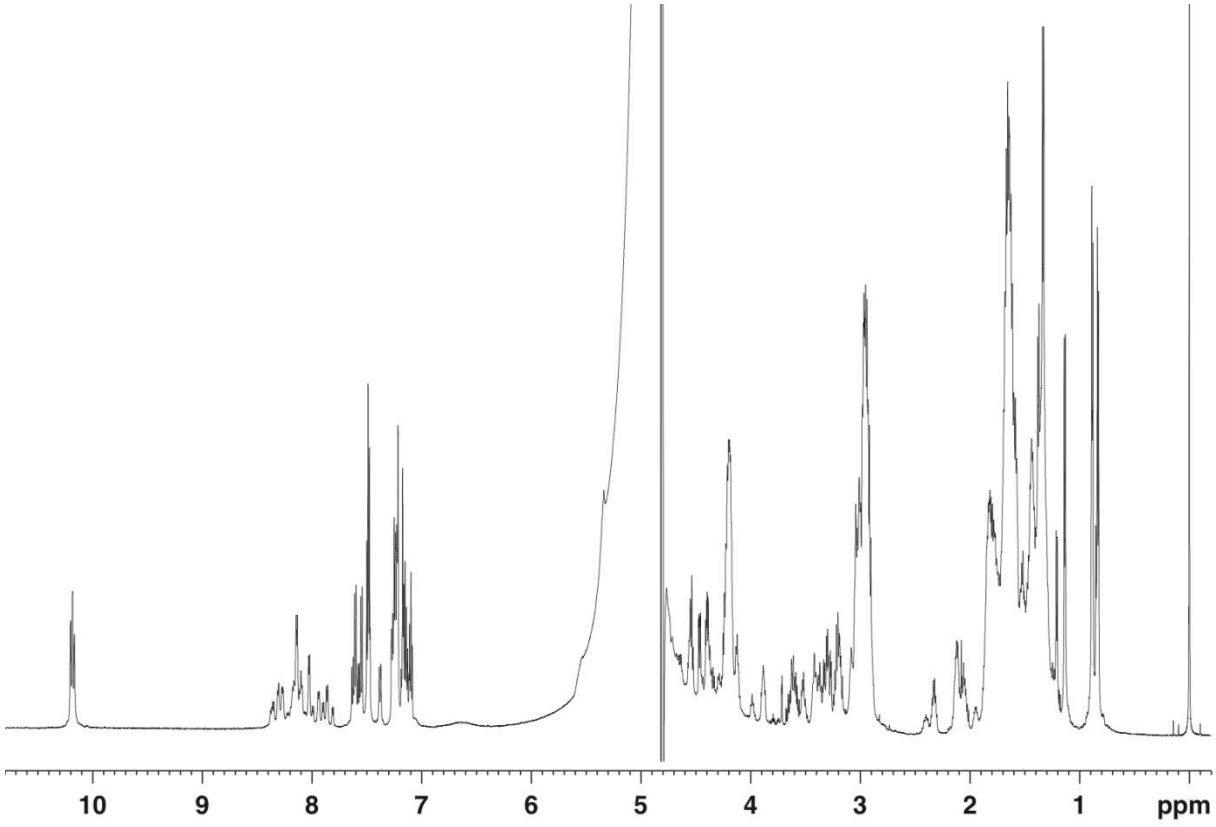

^{1}H-NMR spectrum of **LB-01** (700 MHz, H_2O/D_2O = 9:1, pH 5.0, 298 K).

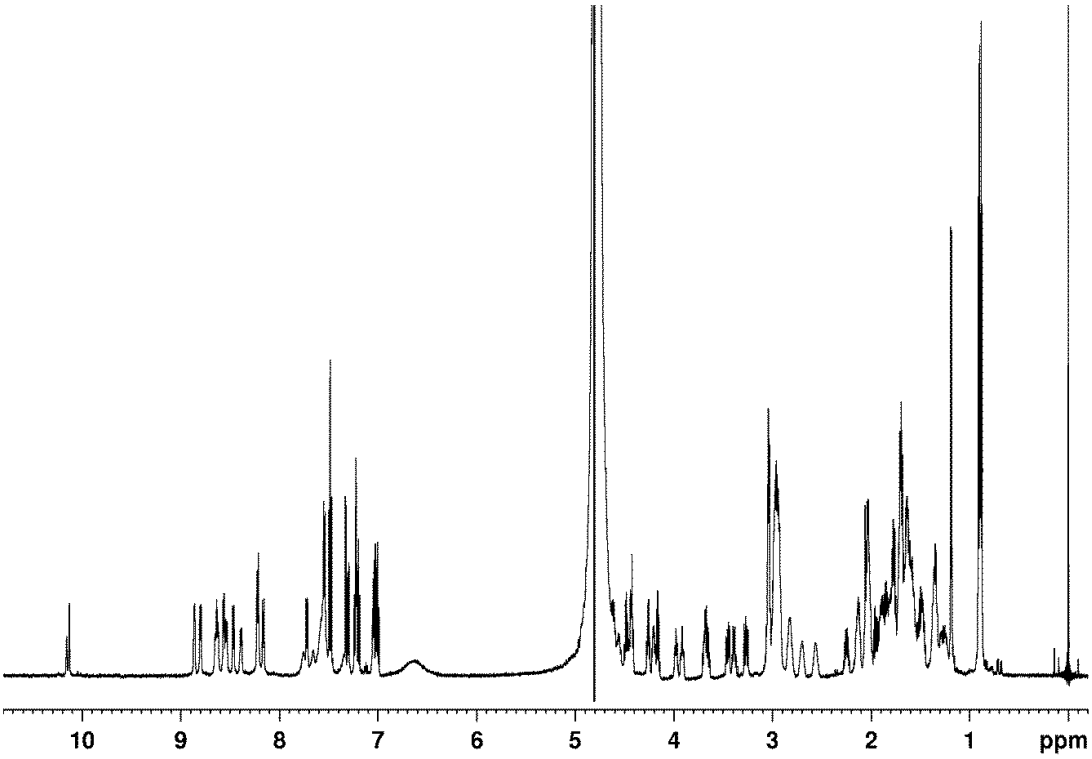

^{1}H-NMR spectrum of **LB-02** (700 MHz, H_2O/D_2O = 9:1, pH 5.0, 298 K).

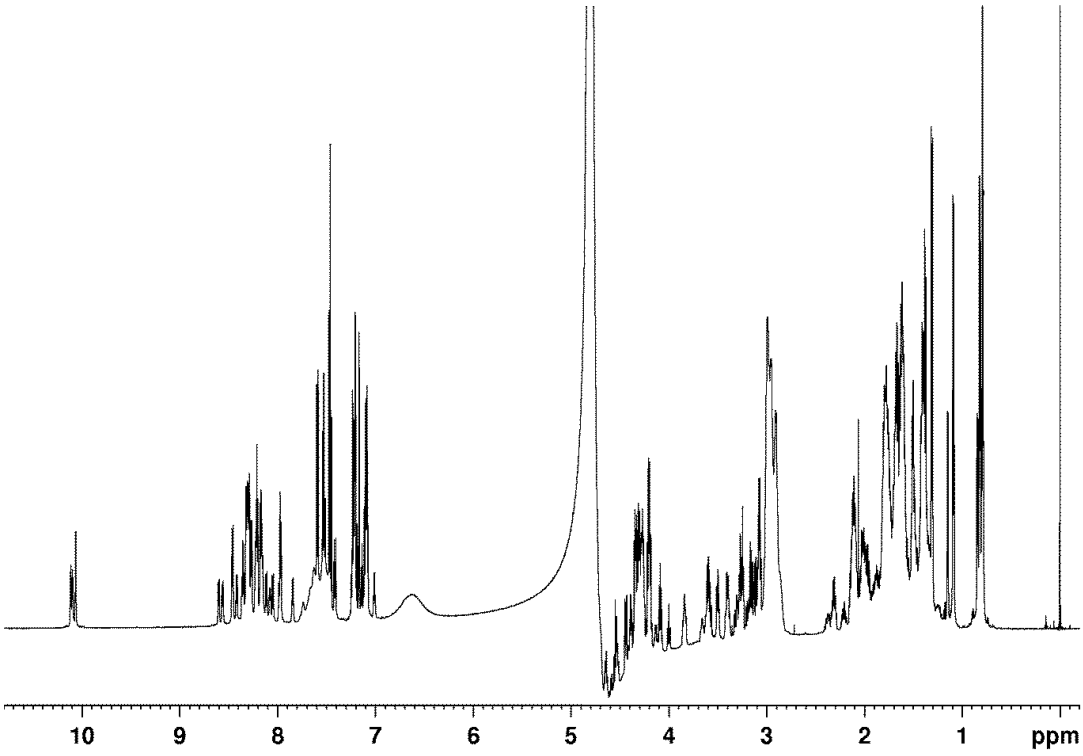

Results from MD simulations. Mean backbone torsion angles ϕ and ψ observed over the course of the restrained MD simulations with **L27-11**, **LB-01** and **LB-02** are shown below:

Peptide		**L27-11**		**LB-01**			**LB-02**	
Residues		Mean (º)	Std.dev		Mean (º)	Std.dev	Mean (º)	Std.dev
Thr[1]	ϕ	-110.1	± 28.7	Thr[1]	-103.9	± 23.0	-69.8	± 14.7
	ψ	157.7	± 23.2		154.7	± 17.9	-21.2	± 12.7
Trp[2]	ϕ	-114.1	± 19.0	Trp[2]	-118.1	± 15.1	-74.4	± 11.9
	ψ	140.3	± 19.9		137.9	± 11.8	-13.4	± 11.0
Leu[3]	ϕ	-101.9	± 18.8	Leu[3]	-93.6	± 12.6	79.1	± 8.8
	ψ	142.4	± 41.4		143.4	± 12.2	-9.1	± 35.0
Lys[4]	ϕ	-152.0	± 5.7	Dab[4]	-141.2	± 12.7	-125.3	± 50.9
	ψ	32.2	± 25.7		138.3	± 9.8	150.3	± 17.9
Lys[5]	ϕ	-75.2	± 17.6	Orn[5]	-142.3	± 10.1	-86.7	± 17.8
	ψ	-24.9	± 15.8		81.3	± 14.9	155.9	± 14.0
Arg[6]	ϕ	-104.1	± 20.7	DLys[6]	75.4	± 11.5	142.5	± 21.5
	ψ	5.4	± 123.8		-123.0	± 10.0	-145.3	± 18.2
Arg[7]	ϕ	2.2	± 79.7	Arg[7]	-81.4	± 12.3	-104.5	± 19.7
	ψ	-12.2	± 40.2		-14.0	± 12.1	112.2	± 32.3
Trp[8]	ϕ	-99.0	± 30.4	Trp[8]	-81.1	± 11.6	-108.1	± 35.5
	ψ	143.7	± 18.6		139.9	± 7.4	132.7	± 38.9
Lys[9]	ϕ	-98.7	± 28.7	Orn[9]	-148.3	± 8.0	-118.2	± 28.1
	ψ	110.9	± 38.6		148.8	± 9.4	-23.3	± 18.2
Lys[10]	ϕ	-125.2	± 25.6	Dab[10]	-148.3	± 9.7	-133.9	± 21.7
	ψ	138.1	± 13.5		140.6	± 8.3	18.8	± 34.6
Ala[11]	ϕ	-83.4	± 14.3	Ala[11]	-78.8	± 10.1	-133.9	± 33.3
	ψ	143.5	± 14.7		146.6	± 9.7	165.7	± 15.6
Lys[12]	ϕ	-136.9	± 12.5	Lys[12]	-135.5	± 11.2	-101.7	± 23.1
	ψ	85.3	± 14.2		81.7	± 10.2	152.5	± 12.5
DPro[13]	ϕ	69.4	± 8.5	*Pro[13]	67.8	± 8.6	-65.9	± 9.3
	ψ	-133.6	± 11.4		-131.1	± 10.3	148.1	± 9.1
Pro[14]	ϕ	-75.9	± 7.7	*Pro[14]	-77.3	± 7.1	80.3	± 6.5
	ψ	-11.4	± 20.2		-11.1	± 18.0	-54.5	± 16.7

* DPro[13] and LPro[14] for **LB-01**; and LPro[13] and DPro[14] for **LB-02**.